Stability of Low-Crested Rubble-Mound Breakwater Heads

By César Vidal,[1] Miguel A. Losada,[2] and Etienne P. D. Mansard[3]

ABSTRACT: Three-dimensional physical models of low-crested, detached rubble-mound breakwaters were built, with their individual sections representing the following components of the breakwater: front slope, crest, back slope, total section (combination of the three previous sections), front head, and back head. The stability of the armor units in each of these sections was assessed, for different freeboards, using irregular waves. In a 1992 paper, Vidal et al. presented the stability criteria for the different trunk sections of this model breakwater. This paper focusses on test results from the head sections. A comparison between the stabilities of the head and trunk sections is also discussed. The stability of the back head (BH) section is found to be highly freeboard-dependent. For fully submerged conditions, the back head is one of the most stable sections of the breakwater. On the other hand, when the breakwater is nonovertopping, it is the least stable section. The front head (FH) section's behavior is similar to that of the front slope section of the breakwater trunk; its stability increases linearly as the freeboard decreases (i.e., as the breakwater becomes immersed).

INTRODUCTION

Low-crested and submerged breakwaters are designed to allow the transmission of a significant amount of wave energy as a result of overtopping. Because of this overtopping, the effects caused by the propagation of waves around the head sections decrease as the freeboard diminishes (freeboard is the elevation of the crest with respect to the still water level). Thus, the weight of the armor stones protecting the head sections can be significantly reduced. A similar weight reduction also applies to the front slope of the trunk section of the breakwater [see Ahrens (1989) and Vidal et al. (1992)].

It is difficult to find studies that describe the stability of submerged breakwater heads from the available literature. In a nonsubmerged situation, many authors have shown that breakwater heads are more prone to damage than their trunk sections [see Iribarren and Nogales (1964), Jensen (1984), and Vidal et al. (1991)]. Grace (1989) reports results of three tests carried out on a nonsubmerged low-crested breakwater. He found that the stability number for zero damage is lower for the head when compared with the stability of other sections. For his tests, the stability number had a value of $0.77X$, in which X is the criteria for zero damage of the total section of the breakwater trunk.

Regarding the propagation of waves around breakwater heads, model studies clearly show that head sections diffract and shoal the waves. In addition, because of the refraction process, the waves focus over the submerged round head and tend to break, forming a jet [see Palmer (1960)]. For nonbreaking waves, the wave-height variation along the head is a function of its size and shape. As the radius of the head relative to wave length increases, the wave height around the head increases, achieving a maximum value near the normal to the wave ray that is tangent to the toe of the head. The precise position of the maximum value depends, according to Losada et al. (1990), on the relative head radius and the head slope. For breaking waves, Vidal et al. (1991) found that the head damage of nonovertopping breakwaters was caused by plunging breakers. Once the units are displaced from their original positions, they move to the lee side by the combined action of flow and gravity. This process has two undesirable effects. First, the units move around into the sheltered area, affecting the navigation channel usually just off the head of the breakwater. Second, these units are no longer available to serve as a seaside berm that could provide a smoother slope to protect the structure. It can be concluded that the head sections of nonovertopping breakwaters are more susceptible to failure than their corresponding trunk sections.

This paper reports on the influence of freeboard on the stability of low-crested breakwater

[1]Assoc. Prof., Dept. de Ciencias y Tecnicas del Agua y del medio Ambiente, Universidad de Cantabria, Avda de los Castros s/n, 39005 Santander, Spain.

[2]Prof., Dept. de Ciencias y Tecnicas del agua y del Medio Ambiente, Universidad de Cantabria, Avda de los Castros s/n, 39005 Santander, Spain.

[3]Sr. Res. Ofcr., Coast. Engrg. Program, Inst. for Engrg. in Can. Environment, Nat. Res. Council Canada, Montreal Rd., Ottawa, Ontario, K1A 0R6 Canada.

heads as measured in laboratory experiments, in the following fashion: first, a description of the experimental setup and measurement techniques is presented. This is followed by a presentation of the analysis of waves and the breakwater damage. Next, a definition of a suitable stability number is discussed. Finally, the results are presented.

EXPERIMENTAL SETUP AND MEASUREMENT TECHNIQUES

Layout of Basin

The physical model tests were carried out in a wave basin, 37 m × 14 m, at the Hydraulics Laboratory of the National Research Council Canada (NRC) in Ottawa, Canada. Fig. 1 shows the experimental setup. A 1.5-m-wide side channel was constructed along one side of the basin to measure the undisturbed incident wave-height distribution. Near the side walls of the remaining 12.5-m-wide channel, modules of upright wave absorbers were placed to dissipate the energy radiated from the head sections of the breakwater. On the end opposite the wave generator, a 1:15 sloped gravel beach was built to ensure an efficient dissipation of wave energy. Except for the gravel beach, the bottom of the basin was horizontal. The breakwater was constructed with its longitudinal axis parallel to the wave board. A distance of approximately 5.5 m between the longitudinal axis of the breakwater and the front toe of the gravel beach was available to monitor the transmitted and diffracted wave energy (see Fig. 1).

The water surface elevations were measured at 11 different locations, as shown in Fig. 1, three of which are in the side channel. One of these gauges was placed close to the wave board in order to monitor the correct reproduction of the desired sea states. For the measurement of reflections, three wave gauges, spaced according to the criterion recommended by Mansard and Funke (1980), were located in front of the model. Three additional gauges were installed in the side channel, at the same distance from the wave board as those installed for reflection measurements in the central section. Four gauges were located between the rear toe of the breakwater and the gravel beach to measure the transmitted waves.

Characteristics of Breakwater

Fig. 2 shows a plan view of the breakwater model. A steel frame covering the upper 0.35 m of the breakwater section was used to subdivide the structure into six components, i.e., four trunk and two head sections. The trunk sections, each 0.5 m wide, consisted of the front slope (FS), back slope (BS), crest (C), and total section (TS). Among the two head sections were the front head (FH), extending over an area covered by an angle of 60° on the front part of one of the heads, and the back head (BH), covering the remaining 120° of the other head. The remaining parts of the breakwater sections, which were not included in these sections, were covered with a wire mesh with square openings of 1 × 1 cm in size. This prevented any motion or damage to these parts of the breakwater, without changing the flow characteristics through and over the structure. This prevented the need to rebuild the entire breakwater after each test.

The breakwater cross section (see Fig. 3) was composed of a permeable core armored with two layers of rocks, which were carefully selected in terms of weight. Some main characteristics of the armor and core stones are provided in Table 1. To ensure easy tracking of the displacement of the armor units, the core and the two layers of the stones were color coded with three different colors. The slopes of all the trunk and head sections were 1:1.5, and the crest width was equivalent to $6D_{n50}$ (where D_{n50} is the nominal diameter of armor stones given by 50% on the diameter distribution curve) and, therefore, approximately 15 cm. D_{n85} and D_{n15} are nominal diameters of stones given by 85% and 15% on the diameter distribution curve. ρ_r is the density of the stone and P_a is the porosity of the layer.
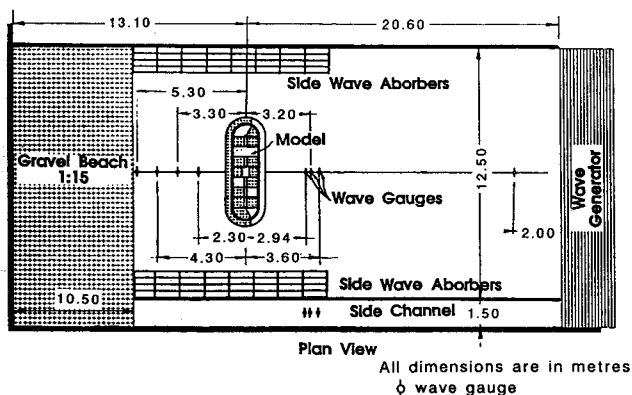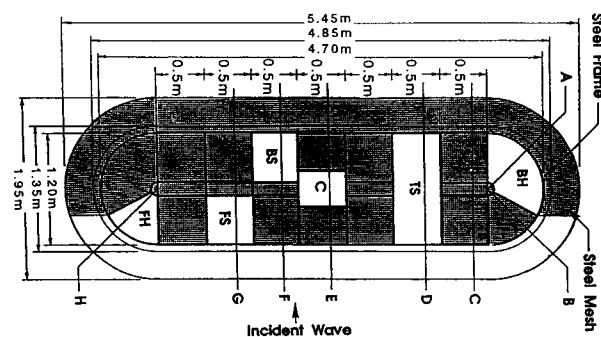

FIG. 1. Plan View of Experimental Setup
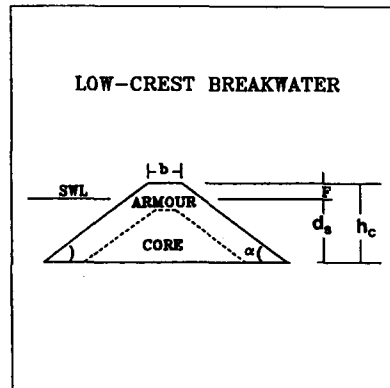

FIG. 2. Plan View of Breakwater Model
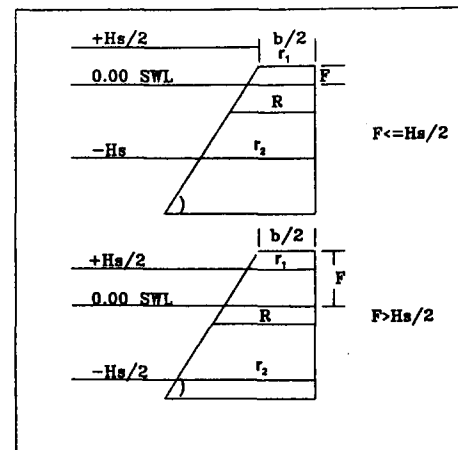
FIG. 3. Cross Section of Low-Crest Breakwater

FIG. 4. Sketch for Damage on Heads

TABLE 1. Model Stone Characteristics

Parameter (1)	Armor (2)	Core (3)
D_{n15}[a]	2.37	1.64
D_{n50}[a]	2.49	1.90
D_{n85}[a]	2.64	2.24
ρ_r[b]	2.65	2.65
P_a	0.45	0.44

[a]In centimeters.
[b]In grams per cubic centimeter.

TABLE 2. Target Parameters for Stability Tests

Test number (1)	d_s (cm) (2)	h_c (cm) (3)	T_p (s) (4)	H_{mo} (cm) (5)
1, 4, 5, 2, 3	40	40	1.4	5, 8, 8, 10, 13
13	60	60	1.4	15
9, 6, 7, 8	45	40	1.4	8, 10, 13, 15
14, 15	65	60	1.4	15, 18
12, 10, 11	38	40	1.4	8, 10, 12
16, 17	58	60	1.4	5, 18
18, 19, 20, 21, 22, 23	56	60	1.4	5, 8, 10, 13, 16, 19
24, 25, 26, 27, 28, 29	54	60	1.4	6, 8, 10, 12, 14, 16
30, 31, 32, 33	58	60	1.8	6, 9, 12, 15
34, 35	54	60	1.8	8, 11

Measurement Techniques and Test Series

To assess the damage and profiles of the sections, video pictures and color photographs were systematically taken before and after each test. Video pictures were also taken during each test to follow the evolution of the damage. The profiling of the breakwater cross sections was performed using an electromechanical profiler with potentiometer sensors, all information being acquired by computer. Nine profiles, 0.05 m apart, were taken for each trunk section. The damage on the head sections was assessed using photographs.

Two repeat sequences of a half-hour time series of irregular waves were used in this study. They were synthesized using the random-phase spectrum method and JONSWAP spectra having a peak enhancement factor of $\gamma = 3.3$. The NRC algorithm used for this purpose is described in Funke and Mansard (1984).

A total of 35 tests was carried out by using two different peak periods ($T_p = 1.4$ s and 1.8 s) and varying the spectrum-based significant wave height H_{mo} at each period. The freeboard was also changed by choosing different water levels. Two different elevations of the structure were made possible by undertaking these investigations in two different wave basins, making sure that the same experimental layout was used in both. The relevant target parameters of these tests are summarized in Table 2. More details on the setup and complete set of results can be found in Vidal and Mansard (1995). The damaged breakwater sections were rebuilt after each test.

DATA ANALYSIS

Wave Data

The wave data from the probes were subjected to spectral, smoothed instantaneous wave energy history (SIWEH) [Funke and Mansard (1979)], zero-crossing, and probability distribution analysis. Reflection analysis, using the method described by Mansard and Funke (1980), was carried out using the data collected from the three probes in front of the test structure. The reflection coefficients estimated by this method can be found in Vidal and Mansard (1995).

Breakwater Damage

The degree of damage on the breakwater was estimated by the following techniques:

- Assessment of damage by a general criterion such as exposure of the first layer; susceptibility of wave attack on the core material, and so on.
- Estimation of a damage parameter based on the number of units displaced. Color photographs and video pictures taken before and after each test were used for this purpose. This parameter will be termed here as visual damage parameter S_v.
- Estimation of a damage parameter S_p based on the eroded area and calculated from profiles of the breakwater sections.

Computation of the last two damage parameters differ slightly for trunk and head sections, because of the difference in their geometries. This aspect is described in the following section.

Trunk Damage

To assess the number of units displaced during each test, color photographs and video pictures were taken before and after the test. If N_{ex} is the number of units displaced in a trunk section of width χ and porosity P_a, the following expression was used to translate this number into an equivalent visual damage parameter, S_v:

$$S_v = \frac{N_{ex} \cdot D_{n50}}{(1 - P_a) \cdot \chi} \tag{1}$$

Using the data from the electromechanical profiler, the average profile for each section of the breakwater before and after each test was calculated, and the average eroded area A_e was derived from profiles. The dimensionless damage parameter S_p was then evaluated from this eroded area using the following expression:

$$S_p = \frac{A_e}{D_{n50}^2} \tag{2}$$

Using the aforementioned two procedures, four values of S_p and S_v corresponding with the four trunk sections were obtained for each test. Based on the experience gained during this comprehensive assessment of damage, it was possible to achieve a critical evaluation of the accuracy and sensitivity of the damage parameters S_v and S_p. For instance, S_p was found to be more accurate when the number of displaced stones N_{ex} was larger than 80. When $N_{ex} < 30$, S_v proved to be more reliable. For situations in which $30 < N_{ex} < 80$, the following approximation was found to be more appropriate:

$$S = aS_v + bS_p \tag{3}$$

where $a = 1 - (N_{ex} - 30)/50$; and $b = (N_{ex} - 30)/50$.

Head Damage

In the head sections, because of their semicircular shape, the number of displaced stones cannot be easily translated to a corresponding value of eroded area. To overcome this difficulty, the following procedure was devised.

Careful observations of the tests showed that the region most prone to damage in the breakwater head is the area between elevations $H_s/2 + SWL$ and $SWL - H_s$, in which H_s is the significant wave height actually measured in the model and SWL denotes the still water level. The head radii r_1 and r_2 correspond with these two extreme elevations. When the freeboard is less than $H_s/2$, r_1 is limited to the radius at the crest elevation (see Fig. 4).

The mean head radius, R, of the damaged area is computed by

$$R = \frac{r_1 + r_2}{2} \tag{4}$$

If α is the angle of the breakwater slope, the following expressions for R can be deduced from Fig. 4 and (4):

$$R = \frac{b}{2} + \frac{\cot \alpha(H_s + F)}{2}, \quad \text{for } F \le \frac{H_s}{2}; \quad R = \frac{b}{2} + \cot \alpha \left(\frac{H_s}{4} + F \right), \quad \text{for } F > \frac{H_s}{2} \quad (5a,b)$$

The arc length $A_{l\theta}$ for a head section covered by θ radians, of mean head radius R, is

$$A_{l\theta} = R\theta \tag{6}$$

If $N_{e\theta}$ represents the number of units displaced in the region covered by an angle θ, the equivalent visual damage parameter for the head section is

$$S_{,h} = \frac{N_{e\theta} \cdot D_{n50}}{(1 - P_a) \cdot A_{l\theta}} \tag{7}$$

In Fig. 2, the total angle covered by the FH section is $\theta = \pi/3$, whereas in the BH section it is equal to $\theta = 2\pi/3$.

Using these criteria, visual damage parameters $S_{,h}$, for the front and back head sections, were computed for each test.

Damage Criteria

Although the aforementioned parameters serve as a good measure for quantifying the degree of damage, they do not provide a physical interpretation of the extent of damage. This interpretation is complicated by the fact that these sections have different geometries. Therefore, it is necessary to define some general damage criteria to relate the physical damage observed in the model with the described parameters.

Losada et al. (1986) defined three different degree of armor damage that can be recognized by visual assessment. These were initiation of damage (ID), Iribarren's damage (IR), and destruction, (D). Vidal et al. (1991) proposed an additional damage level called start of destruction (SD). The definitions of these degrees of damage are as follows:

Initiation of Damage

This level of damage defines the condition attained when a certain number of armor units are displaced from their original position to a new one at a distance equal to or larger than the unit nominal diameter. It also corresponds with the situation in which the outer armor layer displays holes larger than the average pore size on its surface.

Iribarren's Damage

This damage occurs when the extent of the failure area of the outer armor layer is large enough for degrees of waves to act directly on the lower armor layer, with its units susceptible to being displaced.

Start of Destruction

This type of damage is defined as the initiation of damage of the lower layer of the armor, whereby a number of units of the inner armor layer are displaced, causing large holes.

Destruction

Material from the secondary (or filter) layer is removed. If the severity of the sea state does not decrease, the mound will soon cease to give the required level of protection.

The damage criteria for each part of the breakwater was evaluated from a systematic visual inspection of the model after each test. At the end of the test program it was possible to relate these damage levels to the commonly used damage parameter S, which represents the degree of erosion of the structure. These relationships are presented in Table 3.

TABLE 3. Approximate S Values for Different Definitions of Damage

Damage (1)	BH (2)	FH (3)	TS (4)	C (5)	BS (6)	FS (7)
ID	1.0	1.0	1.5	1.0	0.5	1.0
IR	2.0	2.5	2.5	2.5	2.0	2.5
SD	4.0	6.0	6.5	5.0	3.5	4.0
D	9.0	10.0	12.0	10.0	—	9.0

DEFINITION OF SUITABLE STABILITY NUMBER

To establish design criteria for breakwaters, a relationship among the sea state, the mass (or diameter) of the stones, and the level of damage must be established. The wave height of the sea state and the diameter of the stones can be integrated into one overall dimensionless parameter defined as the stability number, N_S. This number is commonly used in the literature and its expression is

$$N_S = \frac{H_{m0}}{\Delta \cdot D_{n50}}. \tag{8}$$

where $\Delta = (\rho_r - \rho)/\rho$ = relative submerged density, ρ_r and ρ = densities of the armor units and water, respectively; and H_{m0} = incident significant wave height estimated from the measured spectra. If the value of this stability number is known for a given damage level, the diameter of the stone that can withstand a given wave height can be easily deduced from the preceding formula. It is relevant to stress that the distortions of wave profiles due to shallow water effects were minimal in this test series. Hence, the values of significant wave height derived either by spectral analysis or by zero-crossing analysis were similar [see Vidal and Mansard (1995)].

The stability results in this study are expressed in terms of freeboard normalized with respect to the nominal diameter of the stone. This normalization is done by the following equation:

$$F_d = F/D_{n50} \tag{9}$$

where F = breakwater freeboard expressed as

$$F = h_c - d_s \tag{10}$$

where h_c = crest height; and d_s = water depth (see Fig. 3).

The damage for a given breakwater should only be a function of the stability number N_S and the normalized freeboard F_d if other parameters such as the water depth, time domain characteristics of incident waves, and sea state duration are all assumed to be constant. This means

$$S = f(N_S, F_d) \tag{11}$$

For any given damage level $S = S_0$ (say initiation of damage), this function can be represented in a two-dimensional plot relating the stability number for this damage level, N_S, with the freeboard by

$$N_S = f_0(F_d) \tag{12}$$

If this function has a minimum value for a certain freeboard, it implies that the freeboard will give the minimum stability for that particular section of the breakwater. As N_S decreases, the wave height H_s, which a stone of nominal diameter D_{n50} can withstand, also decreases.

STABILITY RESULTS OF BREAKWATER HEADS

In the following sections, plots of the stability results (F_d, N_S) will be presented for each of the head sections. Each set of data corresponds to a well defined damage level (see Table 3).

Front Head Section

Fig. 5 presents a plot of the normalized freeboard versus the stability numbers for the FH section of Fig. 2. The straight lines fitted to each data set suggest a linear relationship between the freeboard and the stability number, for each damage level. The minimum value for a given damage level always corresponds with the nonovertopping case of the breakwater. In the case of initiation of damage, this minimum was reached for the maximum freeboard tested. For higher damage levels, the occurrence of minimum stability requires even higher freeboards than those tested here.

The spacing between the lines, representing different damage levels, tends to increase as the freeboard increases. This tendency implies that the FH section is slightly more prone to damage under lower values of freeboard.

During the tests, it was observed that the armor units displaced from this section generally moved down the slope creating a berm, as was seen in the case of the FS section of the breakwater trunk [see Vidal and Mansard (1995)]. Some of the units were carried along with the forward movement of the waves and wound up in the rear of the section. This does not provide any contribution to the improvement of its stability. The cone-shaped head requires more units from the upper levels to be removed in order to provide a berm profile. On the other hand, the down-rush flow is found to be weaker in the FH section than in the FS, because of wave diffraction around the head. As a result, the FH section can be considered to have the same stability as the FS section of the trunk.
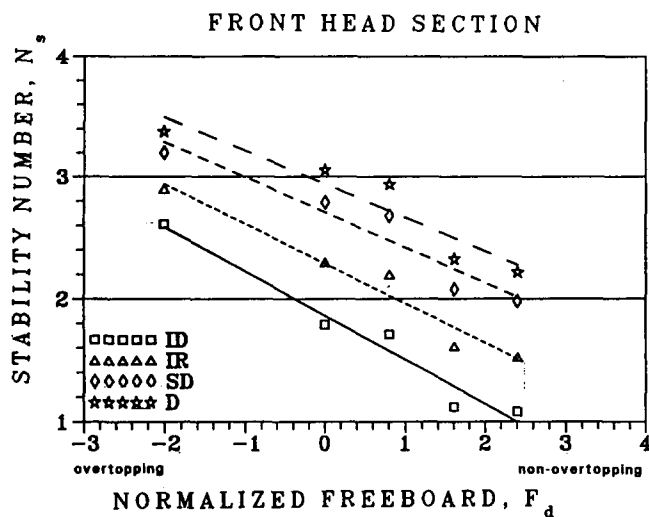
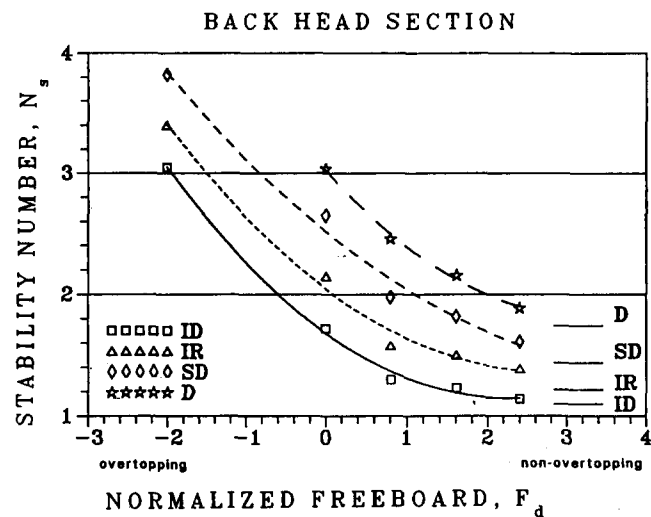FIG. 5. Stability Results for Front Head Section

FIG. 6. Stability Results for Back Head Section

Back Head Section

Fig. 6 presents the stability results for the BH section. The horizontal lines drawn in the lower right-hand corner of the figure correspond with the limiting values of the stability number applicable to the nonovertopping case. These limiting values, presented here for comparison, were taken from the data presented in Vidal et al. (1991). The adaptation of this data to the results of the present study required certain assumptions. The methodology used for this purpose can be found in Vidal and Mansard (1995).

The curves fitted for each damage level are nonlinear. The minimum value in these curves corresponds with the freeboard of nonovertopping, and was reached in the initiation of damage curve for the maximum freeboard tested. For other damage levels, a higher freeboard will have to be included in the testing.

The stability of the BH section increases as the freeboard decreases. The rate of increase in stability (the slope of the curves) rises as the freeboard decreases. As a result, the BH section is very stable for submerged breakwaters, but is the least stable section when it is nonimmersed (or in the nonovertopping situation).

For the highest freeboard tested, the separation between the curves for the initiation of damage and destruction is the shortest for the BH section in comparison with all other breakwater sections tested [see Vidal et al. (1992)]. This means that for high freeboards the BH section is not only the least stable section of the breakwater, but also the one most prone to quick destruction.

In submerged (or overtopping) breakwaters, the waves propagate over the head, and if breaking occurs, it happens over a water cushion. The diffraction over the head makes the flow tangential to the slope. In addition, gravity and flow forces are not in the same direction— which they would be during down rush in a FH section. The movement of displaced units is also possible, starting near the breakwater crest, where the flow is stronger.

For positive freeboards (nonovertopping breakwaters), the diffraction of waves around the head increases the wave height and produces breaking near the intersection of the radius of the head normal to the wave propagation with the water line. This breaking results in a water jet directed downward, which works with the gravity forces to remove armor units from the slope. The armor units are carried down and forward to the back of the head and do not contribute to the protection of this section.

Comparison of Stability between Different Sections

The stability criteria associated with different sections of the breakwater is compared in this section for a given damage level. In this case, the level corresponding with Iribarren's damage is chosen as the representative example.

Fig. 7 plots the stability results (F_d versus N_s) corresponding with Iribarren's damage for all sections of the breakwater. Each set of data corresponds with a different section of the breakwater. The curves representing the head sections are the same as those presented in Figs. 5 and 6. The curves for the trunk sections were extracted from Vidal et al. (1992).

For positive freeboards, the BH section is the least stable. For $F_d > 0$, the BH section has the lowest envelope (least stability) of all the breakwater's sections. Similar findings were established for nonovertopping breakwaters by other researchers.

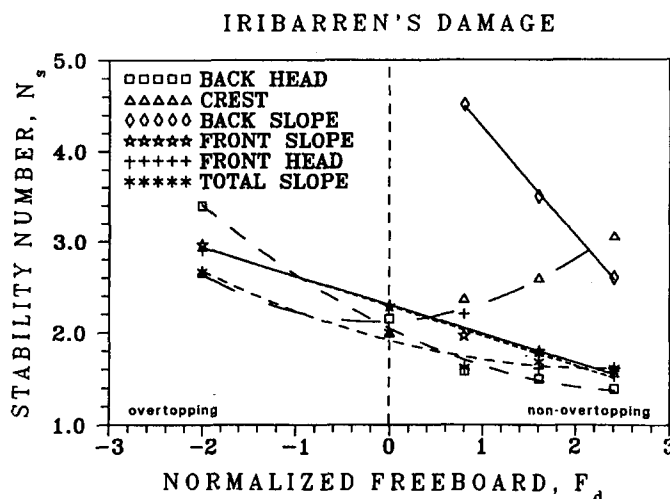Another obvious result is that the BS and BH sections are the most stable sections for fully

IRIBARREN'S DAMAGE

FIG. 7. Comparison among Stability of all Breakwater Sections for Iribarren's Damage

submerged conditions (i.e., $F_d < -1$). It is also clear that the FS section of the trunk and the FH section possess a similar stability behavior, as discussed earlier. Under submerged conditions, the limitation of wave heights due to breaking prevented the occurrence of Iribarren's damage on the back slope.

CONCLUSIONS AND RECOMMENDATIONS

Stability numbers were given for breakwater head sections as a function of the freeboard, for different levels of damage. These criteria can be used to design a stable breakwater head for structures with a relatively porous core.

The stability of low-crested rubble-mound breakwaters was very dependent on the freeboard. This implies that any comparative evaluation of breakwater stability should be based on low levels of damage, such as Iribarren's damage, or lower. Higher values of damage could affect the crest level of the structure and, thereby, the structure's stability and performance characteristics.

The stability of the BH section was highly freeboard-dependent. In a fully submerged situation, it is the most stable section of the breakwater (except for the BS section of the trunk). As the breakwater becomes nonovertopping, the BH section becomes the least stable of all the breakwater sections. It also becomes the most sensitive section for damage. This implies that differences between two different levels of damage is minimal for the BH section of a nonovertopping breakwater.

The FH section behaved in a manner similar to the FS section of the trunk: the stability on the FH section increased linearly as the freeboard decreased. The rate of increase was also similar.

Various sections of the breakwater have different stability responses to a given sea state. If the objective of the model tests is to optimize the armor weight to obtain a similar degree of stability at all sections of the breakwater, the individual stability curves of each section should be taken into consideration. The knowledge of the armor size required for each breakwater section helps optimize the quarry supplies, allowing economically improved breakwater designs.

ACKNOWLEDGMENTS

APPENDIX I. REFERENCES

Ahrens, J. P. (1989). "Stability of reef breakwaters." *J. Wtrwy. Port, Coast. and Oc. Engrg.*, ASCE, 115(2), 221–234.

Desire, J. M. (1985). "Comportamiento de sistemas granulares bajo la accion de flujos oscilatorios. Aplicacion a diques rompeolas de bloques parallelopipedicos," ME thesis, Univ. of Cantabria, Santander, Spain (in Spanish).

Funke, E., and Mansard, E. P. D. (1979). "On the synthesis of realistic sea states in a laboratory flume." *Tech. Rep. LTR-HY-66*, Nat. Res. Council of Canada, Ottawa, Canada.

Funke, E., and Mansard, E. P. D. (1984). "The NRCC 'random' wave package," *Tech. Rep. TR-HY-002* Nat. Res. Council of Canada, Ottawa, Canada.

Grace, P. J. (1989). "Investigation of breakwater stability at Presqu'lsle Peninsula; Erie, Pennsylvania." *Tech. Rep. 89-3*, U.S. Army Corps of Engrs., Coast. Engrg. Res. Ctr. (CERC), Vicksburg, Miss.

Iribarren, R., and Nogales, C. (1964). *Obras Maritimas. Oleaje y Digues*, Dossat, S. A., ed., Madrid, Spain.

Jensen, O. J. (1984). "A monograph on rubble mound breakwaters." Danish Hydr. Inst., Horsholm, Denmark.

Losada, M. A., and Gimenez-Curto, L. A. (1979). "The joint effect of the wave height and period on the stability of rubble mound breakwaters using Iribarren's number." *Coast. Engrg.*, 3(2), 77–96.

Losada, M. A., Dalrymple, R. A., and Vidal, C. (1990). "Water waves in the vicinity of breakwaters." *J. Coast. Res.*, No. 7, 119–138.

Losada, M. A., Desire, J. M., and Alejo, L. M. (1986). "Stability of blocks as breakwater armor units." *J. Struct. Engrg.*, ASCE, 112(11), 2392–2401.

Mansard, E. P. D., and Funke, E. R. (1980). "The measurement of incident and reflected spectra using a least squares method." *Proc., 17th Int. Coast. Engrg. Conf.*, ASCE, New York, N.Y.

Palmer, R. Q. (1960). "Breakwaters in the Hawaiian islands." *J. Wtrwy., Port, Coast., and Oc. Engrg.*, ASCE, 39–67.

Vidal, C., and Mansard, E. P. D. (1995). "On the stability of reef breakwaters." *Tech. Rep.*, National Research Council of Canada, Canada.

Vidal, C., Losada, M. A., and Mansard, E. P. D. (1993). "Suitable wave height parameter for characterizing breakwater stability." *J. Wtrwy., Port, Coast., and Oc. Engrg.*, ASCE, 121(2), 88–97.

Vidal, C., Losada, M. A., and Medina, R. (1991). "Stability of mound breakwater's head and trunk." *J. Wtrwy., Port, Coast., and Oc. Engrg.*, ASCE, 117(6), 570–587.

Vidal, C., Losada, M. A., Medina, R., Mansard, E. P. D., and Gomez-Pina, G. (1992). "A universal analysis for the stability of both low-crested and submerged breakwaters." *Proc., 23rd Int. Coast. Engrg. Conf.*, ASCE, New York, N.Y.

APPENDIX II. NOTATION

The following symbols are used in this paper:

A_e = average eroded area in breakwater transversal section;
$A_{l\theta}$ = arc length in breakwater head;
b = crest width;
D_{n50} = nominal diameter of armor units given by 50% on diameter distribution curve;
d_s = water depth at seaside toe of breakwater;
F = breakwater freeboard before test $(h_c - d_s)$;
F_d = relative freeboard, $Fd = F/D_{n50}$;
H_{m0} = significant wave height derived from spectrum;
H_s = incident significant wave height or average height of largest 1/3 wave heights;
h_c = average crest height of breakwater before wave action measured from seaside toe level;
$N_{e\theta}$ = number of units displaced in region covered by θ;
$N_{e\chi}$ = number of units displaced in trunk section of width χ;
N_S = stability number, $H_{m0}/(\Delta \cdot D_{n50})$;
P_a = porosity;
R = mean head radius;
r_1, r_2 = head radii;
S = average damage parameter;
S_p = damage parameter deduced from profiles;
S_v = visual damage parameter;
S_{vh} = visual damage parameter of head section;
T_p = peak period of spectrum;
α = armor slope angle;
γ = peak enhancement factor of JONSWAP spectrum;
Δ = relative submerged weight $(\rho_r - \rho)/\rho$;
θ = angle covered by head section;
ρ = water density;
ρ_r = mass density of armor units; and
χ = width of trunk section.